Hindawi
Journal of Nanomaterials
Volume 2022, Article ID 6403838, 14 pages
https://doi.org/10.1155/2022/6403838

Research Article

Characterization and Analysis of *Argania spinosa* Shells from Souss-Massa Area: Application in the Adsorption of Methylene Blue in Aqueous Solution

Ousama Ifguis,[1] **Rachid Bouhdadi**,[1] **Younes Ziat**,[2] **Béatrice George**,[3] **and Mohamed Mbarki**[1]

[1]*Engineering Laboratory in Chemistry and Physics of Matter, Faculty of Science and Technics, Sultan Moulay Slimane University, Beni Mellal, Morocco*
[2]*Engineering and Applied Physics Team (EAPT), Sultan Moulay Slimane University, Beni Mellal, Morocco*
[3]*Laboratory of Studies and Research on Material Wood (LERMAB), University of Lorraine, Faculty of Science and Technology, Boulevard des aiguillettes, BP 70239 54506 Vandoeuvre-les-Nancy Cedex, France*

Correspondence should be addressed to Ousama Ifguis; ousama.if@gmail.com

Received 4 January 2022; Revised 4 March 2022; Accepted 12 March 2022; Published 25 March 2022

Academic Editor: Gaurav Sharma

This study focused on the adsorption in aqueous solution of methylene blue (MB), a cationic dye used in the textile industry, by crushed Argan shells (used as raw materials) from the southern region of Morocco. These crushed Argan shells were first characterized by different technical analyses: elemental analysis, biochemical analysis, IR spectroscopy, thermogravimetric analysis, scanning electron microscopy, mercury porosimetry, and zetametry. The adsorption kinetics was then studied by varying the experimental parameters such as the dye concentration in solution. We note that at pH = 8, there is an elimination up to 232.6 mg/g, during an equilibrium time of 180 min. The correlation coefficient showed that the pseudosecond-order kinetic equation best describes the adsorption kinetics for the tested material. The adsorption isotherms of MB by Argan shells are suitably described by the Langmuir model which provide the best theoretical correlation of the experimental data. The thermodynamics of MB adsorption on Argan shells indicates a spontaneous and endothermic process. It was concluded that an increase in temperature leads to a greater adsorption of MB by the studied biosorbent.

1. Introduction

Nowadays, water treatment is a major concern in the context of environmental protection [1]. Industrial wastewater is characterized by the presence of significant amounts of organic and inorganic pollutants, including dyes such as methylene blue [1, 2]. When they are present in river water, the consequences are multiple and harmful: reduction of light penetration due to the coloration of the environment and negative effect on photosynthesis, and these discharges are very difficult to eliminate because of their complex molecular structure [2, 3] and can have dramatic effects on fauna and flora.

The treatment of polluted effluents is of main environmental concern. Whatever the field of application, more constraining laws about the rejected effluents and particularly those contaminated by dyes require the implementation of efficient treatments enabling the recycling of some products and the reuse of purified water mainly in arid countries and desert regions [4].

Among these treatments, we can find those based on flocculation-decantation, ionic exchange, electrolysis, separation on membranes, biological treatments, degradation and adsorption, etc. [5–10].

Nevertheless, the adsorption onto low-cost adsorbents including waste from agriculture or industry and natural

materials appears as one of the most interesting process because of its low cost and ease of implementation. In this context, a lot of studies have been carried out, dealing with, for example, biosorption of heavy metals by olive pomace [11], biosorption of cadmium by bagasse of sugar cane [12], use of cellulosic waste as wheat shells for eliminating methylene blue [13, 14], and acylation of cellulose for lead II adsorption [4].

This present work was aimed at studying the adsorption capacity of Argan shells for removal of methylene blue from aqueous solutions. This dye—in which toxicity increases as the duration of exposure increases—is frequently chosen as a model compound in order to evaluate the removal capacity of the substrates. After the characterization of adsorbent by different techniques, we investigated adsorption kinetics by varying contact time and MB concentrations. The thermodynamic parameters of these adsorption phenomena are also determined to consider further developments.

2. Materials and Methods

2.1. Materials

2.1.1. Adsorbent (Argan Shells). Argan shells used in this study as biosorbents are cheap and highly available lignocellulosic wastes in North Africa. They come more particularly from Souss-Massa-Draâ in the south of Morocco. These wastes are obtained after fruit pulping and crushing to extract pits. Generally, they are not recycled but just degraded by combustion [15].

The dried shells were crushed with a ring grinder (10 s, 1100 rpm) and manually sieved to keep only the size range below 6 mm. The powdered materials were thoroughly washed with distilled water to remove adhering dirt and then dried at 85 ± 5°C in a stove for 24 hours.

Figures 1 illustrate the different stages of Argan shell preparation.

2.1.2. Cationic Dye (Methylene Blue). The methylene blue (or methylthioninium chloride) whose chemical structure is given in Figure 2 is used. The dye is soluble in water and more slightly in alcohol. The methylene blue used in this work was purchased from Janssen Chimica and used without further purification. It was chosen for this study because of its known strong adsorption to solids [16, 17].

2.2. Characterization of the Supports

2.2.1. Elemental Analysis. Final analyses were performed in duplicate on a Thermo Finnigan Flash EA 1112 elemental analyzer equipped with a sample changer and a Porapak chromatographic column. The procedure of this analysis was carried out according to the treatment developed in our previous work [9].

2.2.2. Biochemical Analysis. The biochemical analysis of Argan shells was aimed at determining the quantities: lignin, holocellulose, and extractives found in Argan shells. The determination of the quantities of lignin and holocellulose Klason was made according to the protocols described in the literature [18] and already carried out in our previous work [9]. The determination of the extractives content was done by refluxing a mass of about 2-3 g of ground Argan shells (size less than 6 mm) in a Soxhlet extractor with 350 mL of a 95% (2/1 *v*/*v*) toluene/ethanol solution for 24 hours. Once the solvents were evaporated under vacuum, the percentage of total extractables was deduced from the initial mass m_i and final mass m_f of the dried sample, after drying the samples at 105°C for 48 hours according to

$$\text{Extractives}\% = \frac{m_i - m_f}{m_i} \times 100, \quad (1)$$

where m_i is the initial mass of the dried sample and m_f is the final mass of the dried sample.

2.2.3. Infrared Spectroscopy. For the identification of the different chemical functions of the molecules present in the crushed Argan shells, the latter was analyzed in ATR mode using a spectrophotometer PERKIN ELMER Spectrum 2000 from 400 to 4000 cm^{-1} (16 scans).

2.2.4. Thermogravimetric Analysis. In this study, the apparatus used is the SETARAM Setsys TG 12 thermobalance where a sample of Argan shells (about 80 mg) was introduced. The sample is subjected to a program of temperature increase (5°C min^{-1}) from room temperature to 700°C under a flow of nitrogen (80 mL.min^{-1}) [9–19].

2.2.5. Scanning Electron Microscopy. The Hitachi FEG S 4800 high-resolution electron microscope (resolution of 1 nm and the acceleration voltage was 15 kV) was used in order to obtain SEM images of the ground Argan shells. Before analysis, the dry samples of the ground Argan shells are covered with a layer of carbon to increase their conductivity.

2.2.6. Mercury Porosimetry. Mercury porosimetry was performed on Pascal 140 (Hg pressures < 400 kPa) and Pascal 240 (100 kPa < Hg pressures < 400 MPa) mercury porosimeters from CE Instruments (England). A mass of crushed Argan shells of about (300-350 mg) was introduced into the measuring cell and degassed under vacuum to reach a residual pressure of 0.01 kPa. Then, the measuring cell was filled with mercury. Information on the particle size, bulk density, and specific surface area of the sorbents assuming a cylindrical pore shape is given by the curve giving the intrusion volume of mercury as a function of the applied pressure.

2.2.7. Determination of pH at Zero Charge Point and Measurement of Zeta Potential. To measure pH_{PZC} (pH at the point of zero charge), the method described by Altenor et al. [20] was followed. It consists in placing crushed Argan shells (0.1 g) in 100 mL of a KCl solution at 10^{-2} mol.L^{-1} at various pH values in a pH range from 2 to 12 (solution acidified or basified by hydrochloric acid solution or sodium hydroxide at 0.1 mol.L^{-1}). The final pH (at equilibrium) is measured after 2 days using a pH meter PHM 210 (MeterLab).

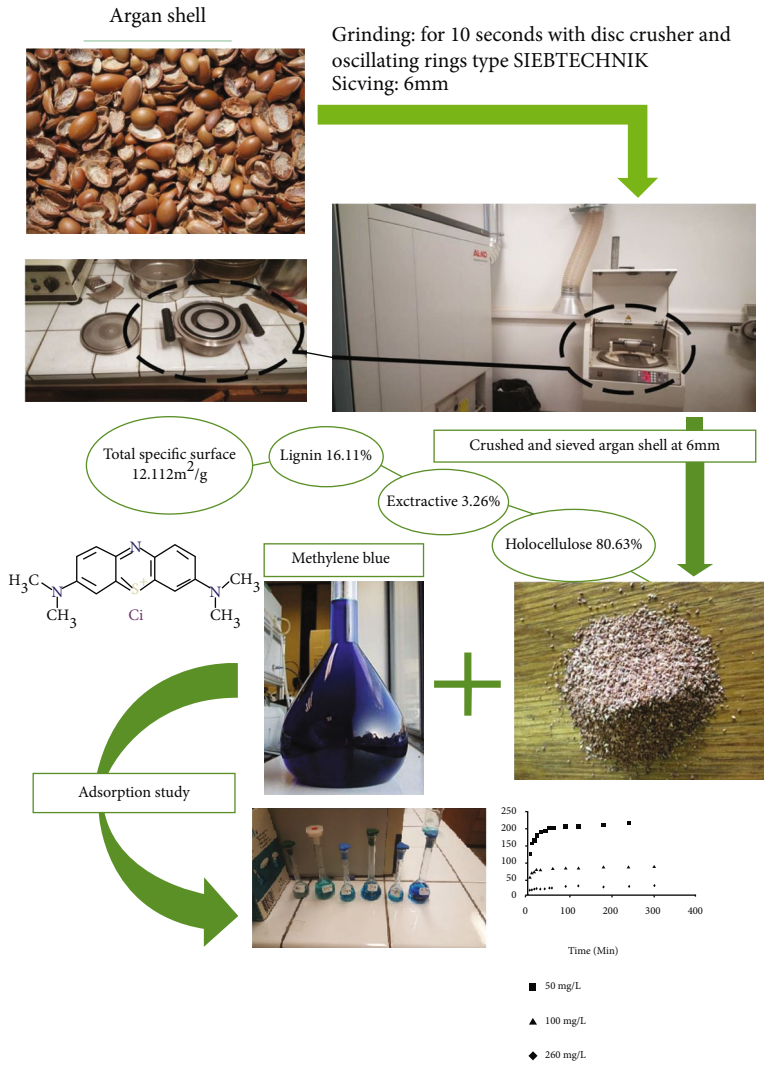

Figure 1: The different stages of preparation of Argan shells.

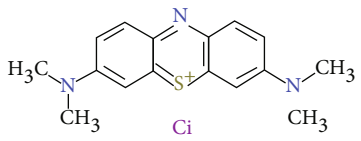

Figure 2: Chemical structure of methylene blue (MB).

Table 1: Elemental analysis of raw Argan shells.

Element	1st measurement	2nd measurement
Carbon	48.13%	47.86%
Hydrogen	5.39%	5.60%
Nitrogen	0.60%	0.53%
Oxygen	40.62%	41.11%
Total	97.74%	95.10%

The zeta potential is a valuable characteristic to understand hydrophilic or hydrophobic properties of materials. The measurements were done using a zetameter Surpass from Anton PAAR. In a first experiment, the zeta potential

Table 2: Biochemical analysis of raw Argan shells.

Compound	Percentage by weight (%)
Lignin	16.11
Holocellulose	80.63
Extractives	3.26

was measured for Argan shells (0.5 g) in contact of different KCl solutions, acidic, basic, or neutral, at 10^{-3} mol.L^{-1}. In a second one, the measurement was carried out in a neutral solution as a function of time.

2.2.8. Adsorption Procedure. The study of the adsorption of MB on Argan shells was performed by mixing a mass of 100 mg of adsorbent in a volume of 100 mL of MB. The working solutions were prepared by dilution from a stock solution of MB (1 g.L^{-1}). The concentrations of the solutions are between 50 and 500 mg.L^{-1}. This mixture was stirred (250 rpm) at room temperature (25 ± 1°C) for the time necessary to reach equilibrium. After separation of the liquid

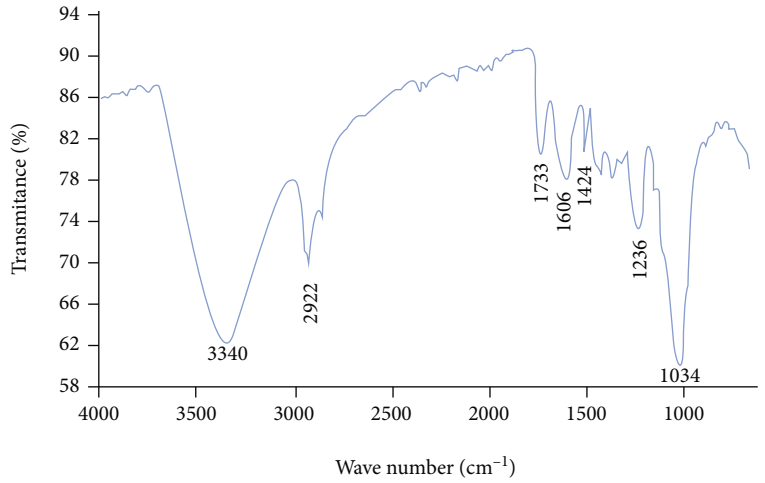

Figure 3: Infrared spectrum of Argan shells in the 4000-400 cm^{-1} spectral region.

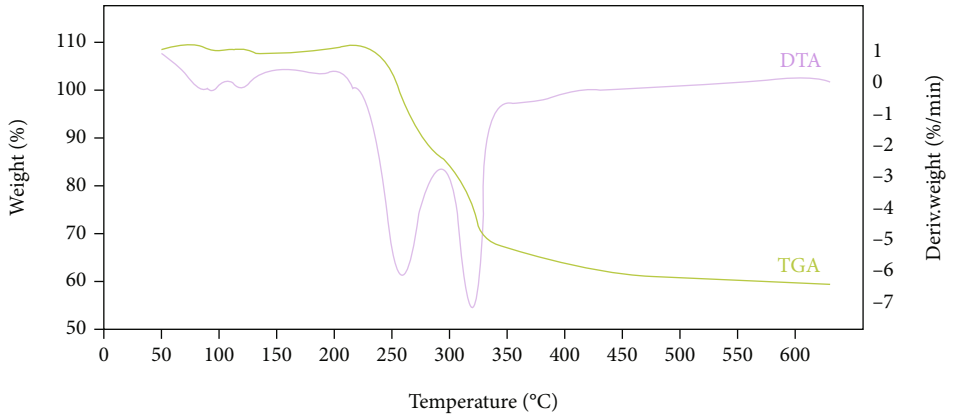

Figure 4: TG/DTA curve analysis of Argan shells at 5°C/min in nitrogen flow (80 $mL.min^{-1}$).

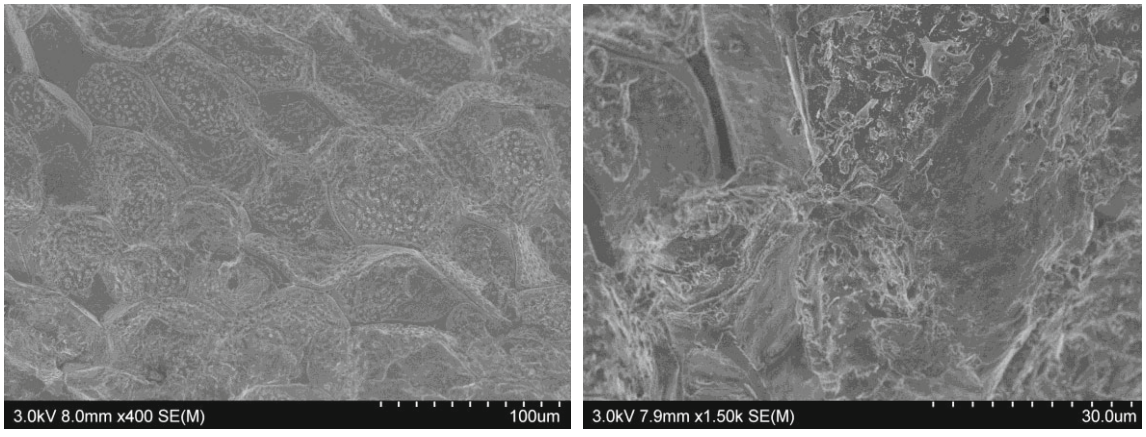

Figure 5: SEM micrograph of Argan shells before adsorption (2 magnifications).

Table 3: Porosity characterization of Argan shells.

Sample	Argan shells
Total cumulative volume (mm^3/g)	288.603
Total specific surface area (m^2/g)	12.112
Average pore diameter (μm)	4.073

Table 4: Evolution of pH for different KCl solutions (100 mL) in contact with Argan shells (mass 0.1 g).

Time (h)	Solution 1	Solution 2	Solution 3	Solution 4	Solution 5
0	1.78	4.17	7.96	9.81	11.43
1	1.50	3.45	6.10	7.92	9.33
2	1.46	2.98	5.34	6.14	7.93
3	1.41	2.10	4.97	5.27	6.34
4	1.36	1.99	4.57	5.01	6.15
5	1.35	1.88	4.39	4.81	6.08
48	1.25	1.77	4.12	4.71	5.97

phase and the adsorbent, the residual concentration of the filtrates was monitored by spectrophotometry in the visible range using a UV-visible spectrophotometer (UV-2550 Shimadzu). The maximum adsorption wavelength of MB is 664 nm.

The equation of the calibration curve is as follows: Absorbance 664 nm = 0.2102 (MB) with MB in $mg.L^{-1}$.

The amount adsorbed is calculated using [9]

$$Q_t = \frac{V \times (C_0 - C_t)}{1000 \times m}, \quad (2)$$

where Q_t is the MB uptake quantity ($mg.g^{-1}$), V is the sample volume (mL), C_0 is the initial MB concentration ($mg.L^{-1}$), C_t is the residual MB concentration ($mg.L^{-1}$), and m is the dry weight of the biosorbent (g).

3. Results and Discussion

3.1. Characterization of Adsorbents. Table 1 illustrates the results of the elemental analysis. The device is equipped to measure carbon, hydrogen, nitrogen, sulfur, and oxygen. The combustion of the sample takes place at high temperature (940°C) in the presence of tungstic anhydride (WO_3) under a current of oxygen for a very short time (15 s). This decomposition gives CO_2, H_2O, SO_2, and NOx; nitrogen oxides are reduced to N_2 (nitrogen) by copper. The whole system is then swept by a current of helium. The (gaseous) combustion products are then measured by gas chromatography (column filled with Chromosorb, katharometer detector) under the conditions determined by the manufacturer and which do not vary. The results are recorded and analyzed by the Eager 300 software. To determine the oxygen content, the samples are pyrolyzed under a stream of helium and the CO formed is quantified by gas chromatography in the stationary phase. Due to the reaction tube filling system, the dosage oxygen cannot be achieved with samples containing fluorine.

Both measurements give similar results: large percentages of carbon and oxygen can be observed because of large amounts of cellulose and lignin precursors in the shells. The differences between 100% and the total correspond to inorganic content (Ca, K, Mg, etc.). The proportions of C, N, and O obtained are in quite good agreement with the values reported in literature for similar lignocellulosic substrates [21, 22].

The biochemical analysis illustrated in Table 2 shows that Argan shells are rich in holocellulose (cellulose+hemicelluloses). The percentage of lignin corresponds to the theoretical percentage reported in literature for this kind of lignocellulosic materials [23]. The extractive content is quite low compared to other biomasses such as orange peels but is quite of the same order as that found for almond peels, for example [9].

Extractives are generally phenolic substances able to interact with cationic dyes, and we could expect acceptable MB adsorption capacity for Argan shells.

FTIR spectra of ground Argan shells are shown in Figure 3 which summarizes the infrared bands in the 4000-400 cm^{-1} spectral region. The IR spectroscopy was aimed at identifying the characteristic functional groups of the adsorbent surface. Generally, these groups are responsible of linkages between adsorbent and adsorbed substance. The spectrum presents the characteristic bands that can be found on IR spectra of cellulose and lignin [24] and are in good agreement with literature [19, 25]. The most intense band in the higher energy region between 3400 and 3200 cm^{-1} is due to a large amount of OH groups in the carbohydrates (carboxyles, phenols, or alcohols) and in adsorbed water [9]. The intense band around 1034 cm^{-1} corresponds to the linkage C-O-H or C-O-R (alcohols or esters), while the band around 2922 cm^{-1} can be assigned to C-H stretching vibration together with bending vibrations around 1424 cm^{-1} of aliphatic chains (-CH_2 and –CH_3) or also methoxyl groups O-CH_3 on which lignocellulosic materials are based. The band around 1733 cm^{-1} corresponds to stretching of C=O groups from ketones, aldehydes, lactones, and carboxylic groups. The band at 1606 cm^{-1} can be attributed to aliphatic and/or unsaturated aromatic compounds and can be correlated to the band at 1236 cm^{-1}. The band at 1606 cm^{-1} could also be attributed to O-H bending in adsorbed water.

Lignocellulosic substrates are complex mix of organic materials, and consequently, thermal treatment produces a variety of chemical and physical changes. Their thermal stability can be studied using thermogravimetric analysis (TGA). Figure 4 shows the thermogravimetric analysis (TGA) and derivative thermogravimetric (DTG) curves of Argan shell sample heated in the conditions described in Materials and Methods. We identify three peaks in the DTG curve and can assign them according to the previous works [26]. We can attribute the first one around 105°C (378 K) to moisture traces release. We assign the second one centered at 287°C (560 K) to the degradation of hemicelluloses and organic and/or aqueous

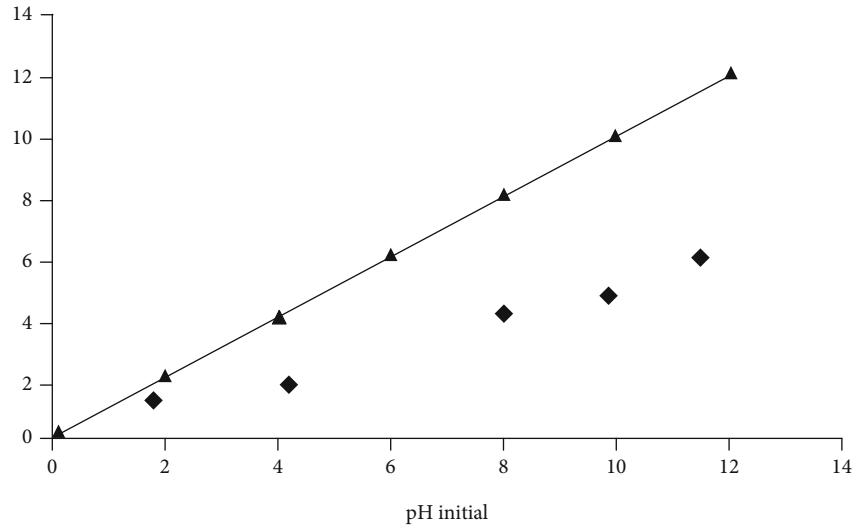

Figure 6: Correlation between initial and final pH values. ◆ Symbols: experimental points; ▲ symbols: theoretical points.

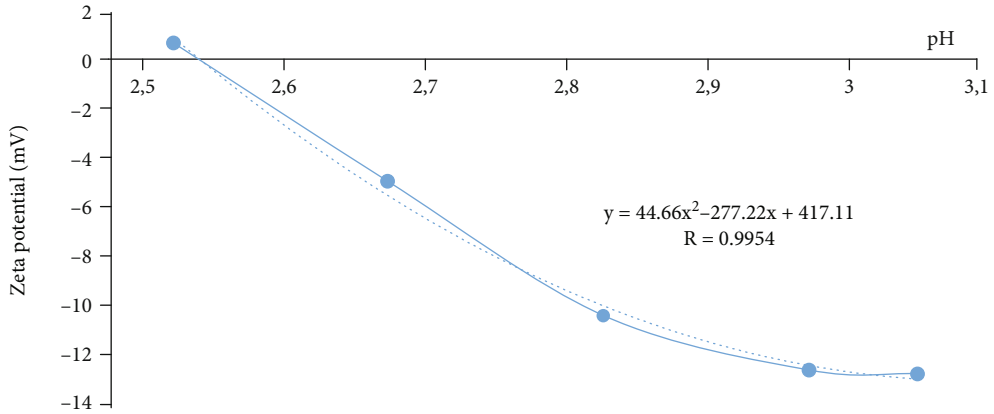

Figure 7: Zeta potential in acid medium.

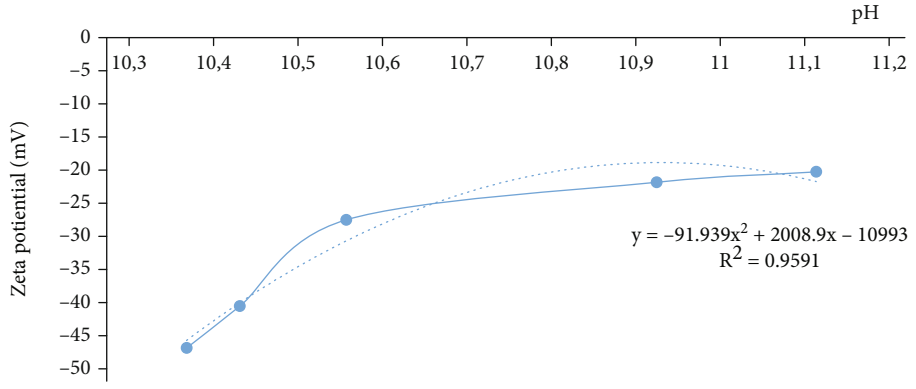

Figure 8: Zeta potential in basic medium.

extractives. The third peak is observed at 355°C (628 K) and corresponds to thermal degradation of cellulose. Above this last temperature, lignin degradation occurs. Our results are in good agreement with those reported in literature on Chinese forest peat or other lignocellulosic materials [27, 28].

The morphology of the samples was characterized before adsorption of MB using SEM, and we present the microphotographs in Figure 5. It can be seen that pores within Argan shells are quite homogeneous and they are well distributed on the sample.

Table 5: Zeta potential over time (raw Argan shells and 1 mM KCl solution).

Time in hours	Zeta potential
0	-24.61
0.5	-20.52
1	-20.68
1.5	-21.16
2	-21.35
18	-22.75

We give the results of porosity measurements in Table 3. Regarding size distribution of particles and porosity of the substrate used, it appears that Argan shells present pores of nearly the same size as almond peels [9], hence a quite interesting specific surface area. By considering that the higher the area, the higher the available adsorption sites, we can assume that the adsorption onto Argan shells should occur in good conditions.

Considering the determination of pH_{PZC} (pH at the point of zero charge) value, the main results obtained are shown in Table 4 and Figure 6.

It appears that pH decreases in a great extent in the first hours of test, particularly in basic solutions and acidic solutions with pH above 4, to finally reach a constant value considered as final pH value. By reporting initial pH values versus final ones, the pH_{PZC} can be estimated to 1.5-2.0 from the extrapolation of the experimental curve to the theoretical one (initial pH = final pH). This means that the surface of the adsorbent is positively charged at pH below 1.5-2.0 and negatively charged for higher pH.

Two experiments were performed with the zetameter. The first was to measure the zeta potential of crushed Argan shells in contact with a solution of potassium chloride to 10^{-3} mol.L^{-1} in acidic, basic, or neutral and the second to measure the zeta potential over time on the same sample of shells at neutral pH.

In acidic medium (Figure 7), it is observed that for a pH < 2.6, the zeta potential becomes positive while beyond, it is negative. The observation of an isoelectric point can reveal the presence of proteins and uronic acids in the lignocellulosic material with pKa between 1.8 and 3 [29].

In a basic medium (Figure 8), the zeta potential is negative but tends to increase as soon as we reach very high pH values (note: measurement problems can occur at such pH values because we reach the limits of use of the Anton PAAR zetameter).

When the potential is measured by passing a neutral KCl solution, it is negative, and we observe that over time, it varies very little, remaining around -20 mV (Table 5). This shows that time is not a factor that influences the zeta potential for our measurements.

On the other hand, a measured negative potential means that the tested material has a hydrophilic character and is subject to swelling [30].

3.2. Adsorption Studies and Modelling

3.2.1. Influence of the Contact Time. Figures 9(a)–9(c) show the evolution of the adsorbed amount of MB as a function of the contact time for different concentrations of MB solutions (50, 100, and 260 mg.L^{-1}) at three different temperatures 25°C, 35°C, and 45°C (298, 308, and 318 K).

We obtained the same kind of curves whatever the concentration used, and we can identify three zones. The first zone is characterized by a very fast adsorption, particularly at low concentrations, as already described [31, 32]. This important increase is followed by a slower adsorption until a stationary state is reached corresponding to approximately 16 mg/g for C = 50 mg.L^{-1} and 206 mg/g for C = 260 mg.L^{-1} after 15 and 180 minutes, respectively (experiment carried out at 25°C).

Increasing temperature generally leads to higher values of adsorbed quantities Q_t at shorter times. For example, Q_t increases from 16 mg/g (25°C) to 36 mg/g (45°C) for C = 50 mg.L^{-1}. An increase of temperature can improve the interactions between adsorbent and dye as already observed and reported in literature [33, 34].

3.2.2. Determination of Rate Constants. In order to approach the real reaction mechanism, we used the modelling of the results obtained. The rate constants for adsorption were determined from simple mathematical models (first order and pseudosecond order) generally used to describe adsorption phenomena for organic compounds onto different substrates [35, 36].

For first-order reaction, the model of Lagergren (1898) [32] gives

$$\log \frac{(Q_e - Q_t)}{Q_e} = -\frac{K_1 \times t}{2.3}. \quad (3)$$

While carrying $\log (Q_e - Q_t)$ versus t, we should obtain a straight line whose slope gives K_1, the rate constant of adsorption (min^{-1}).

For a pseudosecond-order reaction, we deduce the rate constant K_2 from

$$\frac{t}{Q_t} = \frac{1}{2K_2 Q_e^2} + \frac{t}{Q_e}. \quad (4)$$

where, in all the cases, Q_e is the quantity adsorbed at equilibrium (mg/g), Q_t is the quantity adsorbed at time t (mg/g), and t is the time of contact (min).

By plotting t/Q_t versus t, we can determine K_2 (g.min/mg).

Figures 10(a) and 10(b) show the first-order and pseudosecond-order modelling of data corresponding to experimental values obtained from experiments carried out at 25°C (298 K).

From this figure, it appears that the values are best fitted with pseudosecond-order model, and this result was also observed at higher temperatures whatever the concentration. The coefficients of determination are always close to unity ($R^2 > 0,99$) as shown in Table 6 which summarizes all the results deduced from both models (i.e., constants, Q_e, and R^2).

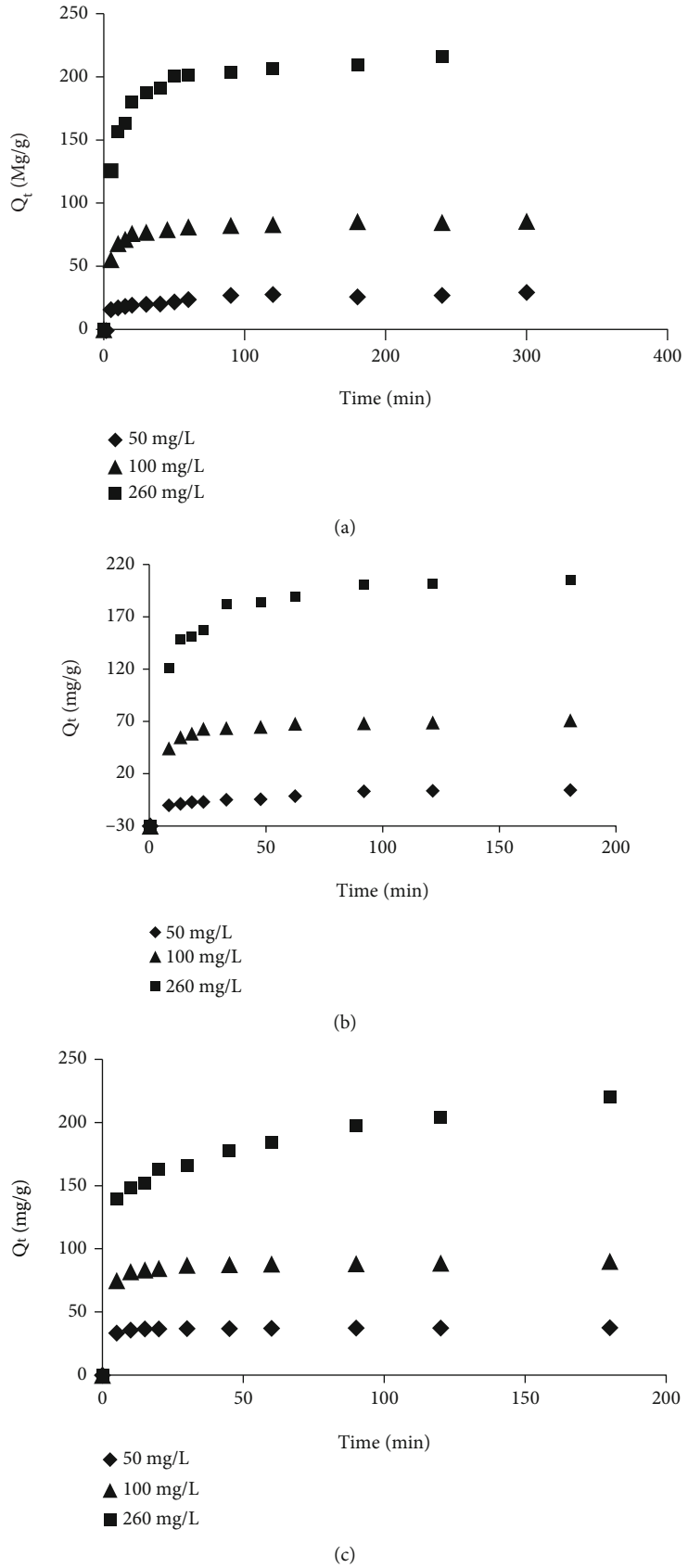

Figure 9: Adsorption of MB onto Argan shells (1 g.L^{-1}) as a function of contact time at different temperatures: (a) 25°C (298 K), (b) 35°C (308 K), and (c) 45°C (318 K).

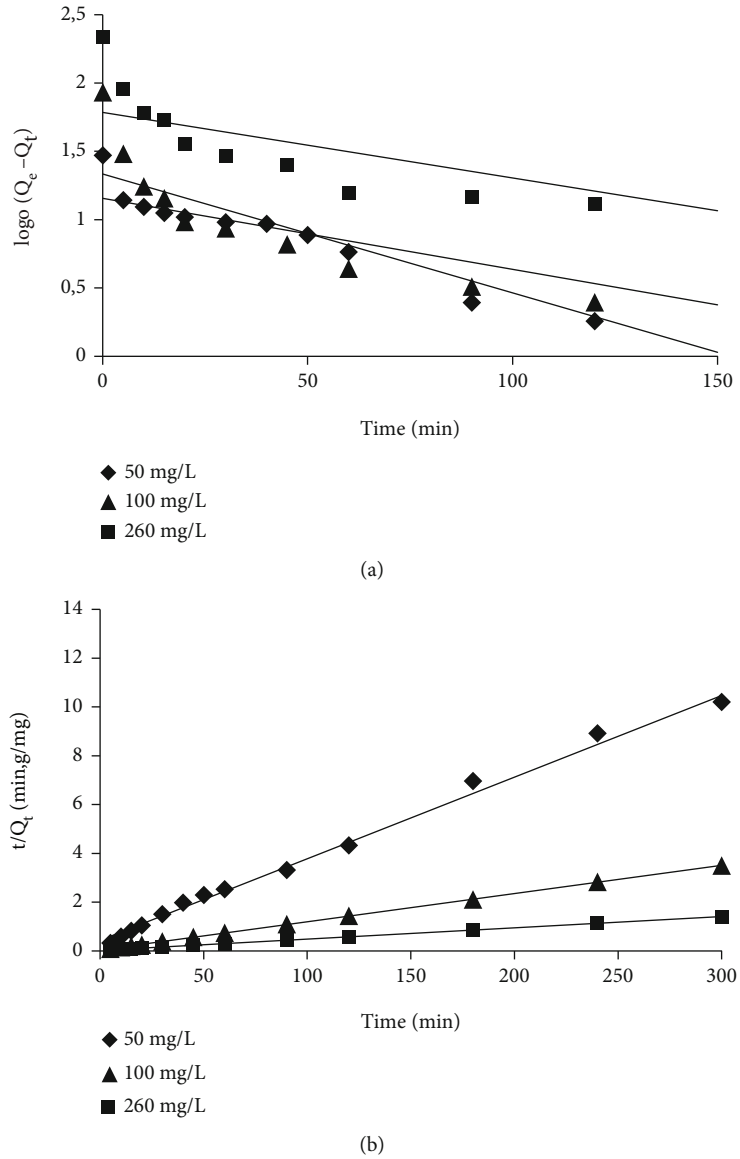

Figure 10: Determination of the rate constant for (a) first-order model and (b) pseudosecond-order model (Argan shells 1 g.L^{-1} at 298 K).

Table 6: Determination of kinetics constants for first and pseudosecond order.

	First order $\mathrm{Log}(Q_e - Q_t) = f(t)$			Pseudosecond order $t/Q_t = f(t)$			
	K_1 (min^{-1})	Q_e calc. (mg/g)	R^2	K_2 (g.min/mg)	Q_e calc. (mg/g)	R^2	
50 mg.L^{-1}	0.01886	17.82	0.757	0.00214	27.77	0.9919	
100 mg.L^{-1}	0.02369	26.04	0.762	0.00172	86.21	0.9999	298 K
260 mg.L^{-1}	0.01104	60.97	0.7078	0.00045	217.39	0.9994	
50 mg. L^{-1}	0.03082	20.13	0.9374	0.00154	31.75	0.9944	
100 mg.L^{-1}	0.02507	21.66	0.7287	0.00231	89.29	0.9998	308 K
260 mg.L^{-1}	0.03059	85.45	0.91	0.00052	212.77	0.9997	
50 mg.L^{-1}	0.03611	3.90	0.7068	0.0213	37.59	1	
100 mg.L^{-1}	0.0253	13.96	0.6241	0.00422	90.09	0.9999	318 K
260 mg.L^{-1}	0.01656	100.95	0.8325	0.000274	222.22	0.9956	

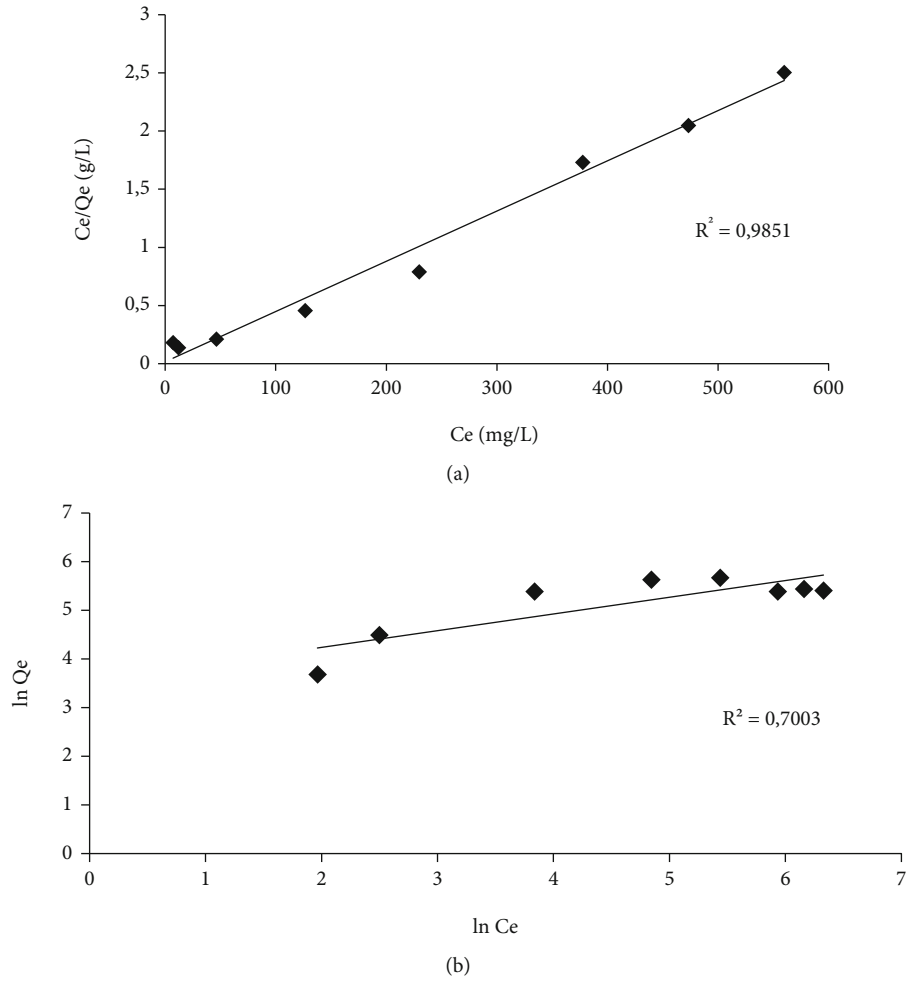

Figure 11: MB adsorption according to (a) Langmuir and (b) Freundlich models on Argan shells (Argan shells 1 g.L^{-1}, temperature 318 K).

Table 7: Maximum amounts adsorbed and constants determined according to Langmuir and Freundlich adsorption models (Argan shells 1 g.L^{-1}, temperature 318 K).

	Langmuir			Freundlich		
	Q_m (mg.g^{-1})	K_L (L.mg^{-1})	$R_L{}^2$	K_F	n	$R_F{}^2$
Argan shells	232.6	0.239	0.9851	34.86	2.91	0.7003

3.2.3. Adsorption Equilibrium. An adsorption isotherm is characterized by constants which give some indications about surface properties and affinity between adsorbate and adsorbent. In our case, the equilibrium data were fitted to the Langmuir and Freundlich isotherm models.

According to Langmuir's model, adsorption occurs through the formation of a monolayer of adsorbate and leads to [37]

$$Q_e = Q_m \times \frac{K_L \times C_e}{1 + K_L \times C_e}, \quad (5)$$

where Q_m is the maximum adsorption capacity (mg/g), K_L is the equilibrium constant, characteristic of the adsorbent (L/mg), depending on temperature and operating conditions, and C_e is the concentration of the adsorbate at equilibrium (mg.L^{-1}).

The Freundlich's model which application is limited to dilute media does not provide an upper limit to the adsorption and admits the existence of interactions between adsorbed molecules [36–38]. It is based on the empirical

$$Q_e = K_F \times (C_e)^{1/n}, \quad (6)$$

where C_e is the concentration of adsorbate at equilibrium (mg.L^{-1}), K_F is the constant related to the adsorption capacity, and n is the heterogeneity factor. In most cases, the adsorption of dye does not follow a simple law.

Figures 11(a) and 11(b) show the modelling of adsorption isotherms of MB using Argan shells according to Langmuir and Freundlich. The Q_m, K_L, and R^2 (coefficient of determination for Langmuir isotherm) and K_F, n, and R^2 (coefficient of determination for Freundlich isotherm) are given in Table 7.

It can be noted that the Freundlich model is not adapted to model the adsorption of MB on the studied crushed

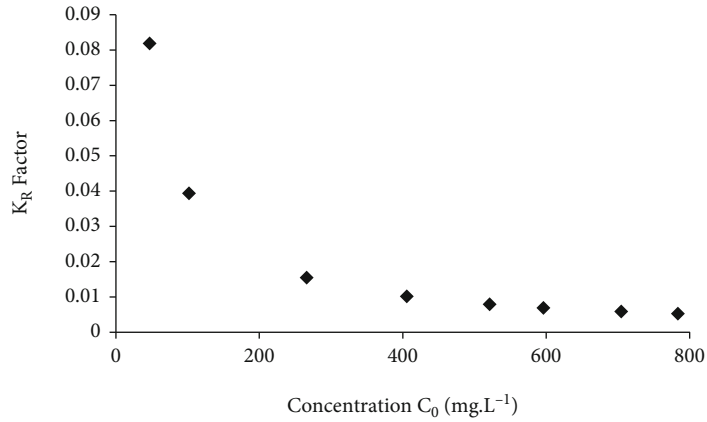

Figure 12: Equilibrium parameter determined by considering a Langmuir model for adsorption on Argan shells (experiments carried out at $T = 298$ K).

Table 8: Thermodynamics associated with adsorption onto Argan shells.

Substrate	ΔH° (kJ/mol)	ΔS° (J/mol/K)	ΔG° (kJ/mol) at 298 K	308 K	318 K	328 K
Argan shells	8.192	42.26	-4.329	-4.506	-5.375	-5.725

Table 9: Comparison of the maximum adsorption capacity of Argan shells with different adsorbents previously reported.

Adsorbent	Maximum adsorption capacity, Q_m (mg/g)	Reference
Typha latifolia	54.73	[40]
Native biochar	106.38	[41]
Strong acid-treated biochar	153.84	[41]
Weak acid-treated biochar	113.63	[41]
Aragn shells	232.6	This work

Argan shells. On the other hand, the Langmuir model is well applicable to the experimental results obtained. For the boyated Argan shells, it seems that the Langmuir model is the most representative of the adsorption mechanism with correlation coefficients worth 0.9851.

We assume that the surface of the biosorbent is covered by a monolayer of dye and the determination of the dimensionless equilibrium parameter $K_R = 1/(1 + K_L C_0)$ with K_L the Langmuir constant (L/mg) and C_0 the initial dye concentration (mg.L^{-1}) which leads to values between 0 and 1 indicating favorable adsorption of MB onto Argan shells. These results are in good agreement with those in literature as several researches carried out on adsorption of cationic dyes onto different cellulosic substrates lead to the same observations [39]. Figure 12 gives the variation of K_R as a function of initial concentration.

3.2.4. Thermodynamic Parameters of Biosorption. To estimate the effect of temperature on the adsorption of MB on Argan shells, thermodynamic parameters were determined from the apparent equilibrium constant K_c of biosorption which is defined as

$$K_c = \frac{(C_0 - C_e)}{C_e}, \tag{7}$$

where $C_0$is the initial concentration (mg.L^{-1}), C_e is the equilibrium concentration (mg.L^{-1}), and K_c is linked to ΔG° hence to ΔH° and ΔS° as follows:

$$\Delta G^\circ = \Delta H^\circ - T\Delta S^\circ = -R.T.\ln(K_c), \tag{8}$$

and consequently leading to

$$\ln(K_c) = -\frac{\Delta H^0}{RT} + \frac{\Delta S^0}{R}, \tag{9}$$

where ΔG° is the standard Gibbs free energy change (J/mol), ΔH° is the standard enthalpy change (J/mol), ΔS° is the entropy change (J/mol.K), R is the universal gas constant (8.314 J/mol.K), and T is the absolute temperature (K).

The plot of ln (K_c) versus $1/T$ leads to values of ΔH° and ΔS°, and the results are given in Table 8.

Whatever the temperature is, the negative values of Gibbs free energy change indicate that the adsorption process is spontaneous. Besides, the positive value of ΔH° shows that it is also endothermic, i.e., the adsorption increases as the temperature increases. The positive value of ΔS° suggests the increased randomness at the solid/solution interface during the adsorption of dye on the sorbent.

The adsorption capacity of Argan shells with respect to methylene blue dye was compared with other adsorbents reported in the literature. The results are grouped together in Table 9.

3.2.5. Methylene Blue Adsorption Mechanism. The possible MB adsorption mechanism onto lignocellulosic biomass (Argan shells) is schematically illustrated in Figure 13.

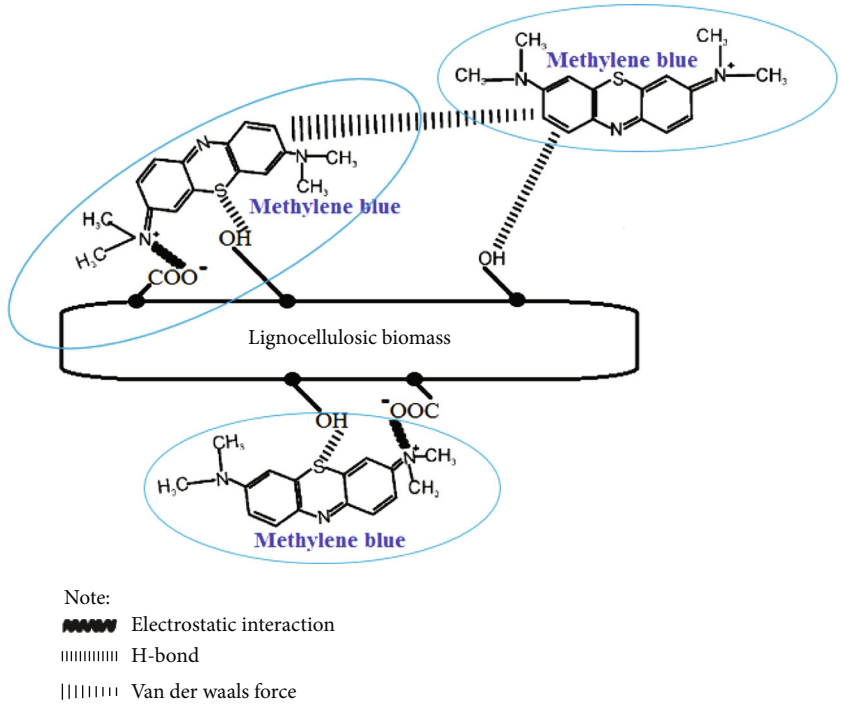

Figure 13: Possible MB adsorption mechanism onto lignocellulosic biomass (Argan shells).

The mechanism of adsorption techniques involves four steps: migration of dye molecules from the bulk solution to the sorbent surface, diffusion through the boundary layer to the sorbent surface, adsorption at a single site, and intraparticle diffusion onto the sorbent [42]. Figure 13 represents the possible mechanism of MB adsorption on lignocellulosic biomass (Argan shells). The adsorption capacity depends on the structural and functional behavior of the sorbent. MB can be readily adsorbed to lignocellulosic bioadsorbents by forces such as van der Waals force and hydrogen bonding interactions [43, 44].

According to biochemical analysis, Argan shells are rich in cellulose which consists of -OH groups, arranged in a sequence based on β-D-glucopyranose-1,4-β-D-glucopyranose. The binding between the cellulose-rich adsorbent (Argan shells) and methylene blue can be achieved by hydrogen bonds and van der Waals bonds.

4. Conclusion

In this study, we first analyzed Argan shells by different techniques (elemental analysis, biochemical analysis, FTIR, thermogravimetric analysis, scanning electron microscopy, mercury porosimetry, and zetametry) and then used them as potential biosorbent. It appears that this substrate is efficient for eliminating MB from aqueous solutions. The monolayer adsorption capacity was estimated to 232.6 mg/g. The adsorption process depends on contact duration, and equilibrium is reached after 180 minutes. In this study, it appears that the adsorption kinetics are well described by a pseudosecond-order model and that the process is conveniently modelled by a Langmuir model. The determination of thermodynamic parameters shows that the adsorption spontaneously occurs onto the substrate and is all the more favored than temperature increases since the process is endothermic.

Data Availability

The data used to support the findings of this study are included within the article.

Conflicts of Interest

The authors declare that they have no known competing financial interests or personal relationships that could have appeared to influence the work reported in this paper.

Authors' Contributions

Ousama Ifguis proposed the idea, supervised the study, wrote the manuscript, and prepared and analyzed the data. Younes Ziat helps in editing and paper correction. Rachid Bouhdadi was responsible for the analysis of the data and interpretation. Mohamed Mbarki was responsible for the correction of the document and interpretation. Béatrice George was responsible for the laboratory support, writing, analysis of the data, and interpretation. All authors contributed in the final version.

References

[1] S. Shivalkar, P. K. Gautam, S. Chaudhary, S. K. Samanta, and A. K. Sahoo, "Recent development of autonomously driven micro/nanobots for efficient treatment of polluted water," *Journal of Environmental Management*, vol. 281, article 111750, 2021.

[2] A. K. Degbe, M. Koriko, S. Tchegueni et al., "Biosorption of methylene blue solution: comparative study of the cactus (Opuntia ficusindica) of Lmé (CL) and Marrakech (CM)," *Journal of Materials and Environmental Science*, vol. 7, pp. 4786–4794, 2016.

[3] T. Madrakian, A. Afkhami, H. Mahmood-Kashani, and M. Ahmadi, "Adsorption of some cationic and anionic dyes on magnetite nanoparticles-modified activated carbon from aqueous solutions: equilibrium and kinetics study," *Journal of the Iranian Chemical Society*, vol. 10, no. 3, pp. 481–489, 2013.

[4] E. Forgacs, T. Cserhati, and G. Oros, "Removal of synthetic dyes from wastewaters: a review," *Environment International*, vol. 30, no. 7, pp. 953–971, 2004.

[5] R. Bouhdadi, M. El Moussaouiti, B. George, S. Molina, and A. Merlin, "Acylation de la cellulose par le chlorhydrate de chlorure de 3-pyridinoyl: application dans l'adsorption du plomb Pb2+," *Comptes Rendus Chimie*, vol. 14, no. 6, pp. 539–547, 2011.

[6] Q. Liu, Y. Li, H. Chen et al., "Superior adsorption capacity of functionalised straw adsorbent for dyes and heavy-metal ions," *Journal of Hazardous Materials*, vol. 382, article 121040, 2020.

[7] S. Q. Badr and F. A. Sahib, "Effect of incubation time on copper uptake and biomass of aspergillus terreus," *Assiut University Bulletin for Environmental Researches*, vol. 23, no. 2, 2020.

[8] G. Sharma, D. D. Dionysiou, S. Sharma et al., "Highly efficient Sr/Ce/activated carbon bimetallic nanocomposite for photoinduced degradation of rhodamine B," *Catalysis Today*, vol. 335, pp. 437–451, 2019.

[9] G. Sharma, A. Kumar, S. Sharma et al., "Fe_3O_4/ZnO/Si_3N_4 nanocomposite based photocatalyst for the degradation of dyes from aqueous solution," *Materials Letters*, vol. 278, article 128359, 2020.

[10] V. Bharti, K. Vikrant, M. Goswami et al., "Biodegradation of methylene blue dye in a batch and continuous mode using biochar as packing media," *Environmental Research*, vol. 171, pp. 356–364, 2019.

[11] N. Saha, M. Volpe, L. Fiori, R. Volpe, A. Messineo, and M. T. Reza, "Cationic dye adsorption on hydrochars of winery and citrus juice industries residues: performance, mechanism, and thermodynamics," *Energies*, vol. 13, no. 18, p. 4686, 2020.

[12] M. E. Peñafiel, J. M. Matesanz, E. Vanegas, D. Bermejo, R. Mosteo, and M. P. Ormad, "Comparative adsorption of ciprofloxacin on sugarcane bagasse from Ecuador and on commercial powdered activated carbon," *Science of the Total Environment*, vol. 750, article 141498, 2021.

[13] M. Boumediene, H. Benaïssa, B. George, S. Molina, and A. Merlin, "Characterization of two cellulosic waste materials (orange and almond peels) and their use for the removal of methylene blue from aqueous solutions," *Maderas. Ciencia y Tecnología*, vol. 17, no. ahead, 2015.

[14] H. Chandarana, S. K. Ponnusamy, S. Muthulingam, and A. K. Madhava, "Kinetics, equilibrium and thermodynamic investigations of methylene blue dye removal using Casuarina equisetifolia pines," *Chemosphere*, vol. 285, article 131480, 2021.

[15] K. R. Hakeem, M. Jawaid, and O. Y. Alothman, *Agricultural biomass based potential materials*, Springer International Publishing Switzerland, 2015.

[16] H. Dai, Y. Huang, and H. Huang, "Eco-friendly polyvinyl alcohol/carboxymethyl cellulose hydrogels reinforced with graphene oxide and bentonite for enhanced adsorption of methylene blue," *Carbohydrate Polymers*, vol. 185, pp. 1–11, 2018.

[17] M. J. Ahmed and S. K. Dhedan, "Equilibrium isotherms and kinetics modeling of methylene blue adsorption on agricultural wastes-based activated carbons," *Fluid Phase Equilibria*, vol. 317, pp. 9–14, 2012.

[18] M. A. Xiaojuan, X. Yang, X. Zheng et al., "Toward a further understanding of hydrothermally pretreated holocellulose and isolated pseudo lignin," *Cellulose*, vol. 22, no. 3, pp. 1687–1696, 2015.

[19] R. Bilbao, J. F. Mastral, M. E. Aldea, and J. Ceamanos, "The influence of the percentage of oxygen in the atmosphere on the thermal decomposition of lignocellulosic materials," *Journal of Analytical and Applied Pyrolysis*, vol. 42, no. 2, pp. 189–202, 1997.

[20] S. Altenor, B. Carene, E. Emmanuel, J. Lambert, J. J. Ehrhardt, and S. Gaspard, "Adsorption studies of methylene blue and phenol onto vetiver roots activated carbon prepared by chemical activation," *Journal of Hazardous Materials*, vol. 165, no. 1-3, pp. 1029–1039, 2009.

[21] L. Lü, L. Chen, W. Shao, and F. Luo, "Equilibrium and kinetic modeling of Pb (II) biosorption by a chemically modified orange peel containing Cyanex 272," *Journal of Chemical & Engineering Data*, vol. 55, no. 10, pp. 4147–4153, 2010.

[22] B. Zapata, J. Balmaseda, E. Fregoso-Israel, and E. Torres-Garcia, "Thermo-kinetics study of orange peel in air," *Journal of Thermal Analysis and Calorimetry*, vol. 98, no. 1, pp. 309–315, 2009.

[23] G. N. Inari, M. Petrissans, and P. Gerardin, "Chemical reactivity of heat-treated wood," *Wood Science and Technology*, vol. 41, no. 2, pp. 157–168, 2007.

[24] H. Yang, R. Yan, H. Chen, D. H. Lee, and C. Zheng, "Characteristics of hemicellulose, cellulose and lignin pyrolysis," *Fuel*, vol. 86, no. 12-13, pp. 1781–1788, 2007.

[25] X. Li, Y. Tang, X. Cao, D. Lu, F. Luo, and W. Shao, "Preparation and evaluation of orange peel cellulose adsorbents for effective removal of cadmium, zinc, cobalt and nickel," *Colloids and Surfaces A: Physicochemical and Engineering Aspects*, vol. 317, no. 1-3, pp. 512–521, 2008.

[26] S. Soares, G. Camino, and S. Levchik, "Comparative study of the thermal decomposition of pure cellulose and pulp paper," *Polymer Degradation and Stability*, vol. 49, no. 2, pp. 275–283, 1995.

[27] H. Chen, W. Zhao, and N. Liu, "Thermal analysis and decomposition kinetics of Chinese forest peat under nitrogen and air atmospheres," *Energy & Fuels*, vol. 25, no. 2, pp. 797–803, 2011.

[28] A. G. Barneto, R. B. Hernández, and J. M. Berenguer, "Thermogravimetric characterization of eucalyptus wood," *O PAPEL*, vol. 72, no. 7, pp. 53–56, 2011.

[29] A. Baltazar-y-Jimenez and A. Bismarck, "Wetting behaviour, moisture up-take and electrokinetic properties of lignocellulosic fibres," *Cellulose*, vol. 14, no. 2, pp. 115–127, 2007.

[30] A. Bismarck, I. Aranberri-Askargorta, J. Springer et al., "Surface characterization of flax, hemp and cellulose fibers; surface properties and the water uptake behavior," *Polymer Composites*, vol. 23, no. 5, pp. 872–894, 2002.

[31] K. Sudalyandi, *Equilibrium and Kinetic Studies of Freon-14 Adsorption onto Porous Solids under Elevated Pressure*, Illinois Institute of Technology, 1996.

[32] K. E. Noll, V. Gounairis, and W. S. Hou, "Adsorption theory," in *Adsorption Technology for Air and Water Pollution Control*, p. 21, CRC Press, 2nd edition, 1991.

[33] M. Doğan, M. Alkan, Ö. Demirbaş, Y. Özdemir, and C. Özmetin, "Adsorption kinetics of maxilon blue GRL onto sepiolite from aqueous solutions," *Chemical Engineering Journal*, vol. 124, no. 1-3, pp. 89–101, 2006.

[34] A. E. Ofomaja, "Sorptive removal of methylene blue from aqueous solution using palm kernel fibre: effect of fibre dose," *Biochemical Engineering Journal*, vol. 40, no. 1, pp. 8–18, 2008.

[35] S. K. Lagergren, "About the theory of so-called adsorption of soluble substances," *Sven. Vetenskapsakad. Handingarl*, vol. 24, pp. 1–39, 1898.

[36] Y. S. Ho and G. McKay, "Pseudo-second order model for sorption processes," *Process Biochemistry*, vol. 34, no. 5, pp. 451–465, 1999.

[37] K. V. Kumar and K. Porkodi, "Relation between some two- and three-parameter isotherm models for the sorption of methylene blue onto lemon peel," *Journal of Hazardous Materials*, vol. 138, no. 3, pp. 633–635, 2006.

[38] C. H. Yang, "Statistical mechanical study on the Freundlich isotherm equation," *Journal of Colloid and Interface Science*, vol. 208, no. 2, pp. 379–387, 1998.

[39] L. Yu and Y. M. Luo, "The adsorption mechanism of anionic and cationic dyes by Jerusalem artichoke stalk-based mesoporous activated carbon," *Journal of Environmental Chemical Engineering*, vol. 2, no. 1, pp. 220–229, 2014.

[40] A. El Amri, J. Bensalah, A. Idrissi et al., "Adsorption of a cationic dye (Methylene bleu) by Typha Latifolia: equilibrium, kinetic, thermodynamic and DFT calculations," *Collections*, vol. 38, article 100834, 2022.

[41] A. B. Albadarin, M. N. Collins, M. Naushad, S. Shirazian, G. Walker, and C. Mangwandi, "Activated lignin-chitosan extruded blends for efficient adsorption of methylene blue," *Chemical Engineering Journal*, vol. 307, pp. 264–272, 2017.

[42] N. A. Oladoja, C. O. Aboluwoye, Y. B. Oladimeji, A. O. Ashogbon, and I. O. Otemuyiwa, "Studies on castor seed shell as a sorbent in basic dye contaminated wastewater remediation," *Desalination*, vol. 227, no. 1-3, pp. 190–203, 2008.

[43] O. Üner, Ü. Geçgel, and Y. Bayrak, "Adsorption of methylene blue by an efficient activated carbon prepared from Citrullus lanatus rind: kinetic, isotherm, thermodynamic, and mechanism analysis," *Water, Air, & Soil Pollution*, vol. 227, no. 7, pp. 1–15, 2016.

[44] S. Manna, D. Roy, P. Saha, D. Gopakumar, and S. Thomas, "Rapid methylene blue adsorption using modified lignocellulosic materials," *Process Safety and Environmental Protection*, vol. 107, pp. 346–356, 2017.